JOURNAL OF GUIDANCE, CONTROL, AND DYNAMICS
Vol. 16, No. 2, March-April 1993

Active Vibration Damping of the Space Shuttle Remote Manipulator System

Michael A. Scott* and Michael G. Gilbert†
NASA Langley Research Center, Hampton, Virginia 23665
and
Martha E. Demeo‡
Charles Stark Draper Laboratory, Cambridge, Massachusetts 02139

Controls-structures interaction is a technology currently under development for application to large flexible space vehicles. The goal of this technology is the improvement of spacecraft performance through active control of the structural dynamic response of the vehicle. This goal is particularly important for modern spacecraft designs where large size and reduced stiffness make structural response a significant contributor to vehicle dynamics. Analysis and design methods have been developed to analyze and predict flexible spacecraft performance, but the technology remains largely unvalidated by hardware experiments, demonstrations, or applications, particularly in-space flight applications. One potential application considered is to provide active damping augmentation of the Space Shuttle remote manipulator system. The objective of actively damping the manipulator is to demonstrate improved structural dynamic response following payload maneuvers and Shuttle reaction control system thruster firings. This paper describes an initial analysis effort to determine the feasibility of controlling the flexible dynamic response of the arm. The approach to the study is summarized and results from both linear and nonlinear performance analyses of candidate control laws are presented. Results indicate that significant improvement in dynamic response can be achieved through active control if measured arm tip acceleration was made available for feedback.

I. Introduction

THIS paper describes the ongoing analysis effort to determine the feasibility of providing active damping augmentation of the Space Shuttle remote manipulator system (RMS) following normal payload handling operations. The RMS exhibits long periods of oscillatory motion following routine operational maneuvers.[1] The effort is motivated in part by a study completed by the Charles Stark Draper Laboratory (CSDL) in June 1989.[2,3] The flight experiment study suggested adding additional sensors to the arm, the installation of a flight experiment computer and hardware in the Shuttle cargo bay, and the use of an instrumented payload at the end of the arm to measure performance. A study of RMS active damping augmentation benefits for the assembly of a strut truss Space Station Freedom (SSF) design also motivated the current effort.[4] This study determined that approximately 10 h of cumulative time would be spent over 15 SSF-assembly Shuttle flights waiting for arm tip motion to damp down to within ±1 in. amplitudes following maneuvers with SSF components. The study also showed that a simple two-fold increase in the level of damping of the arm could reduce the cumulative settling time to 4 h, a reduction in time approximately equal to the programmed arm-operation time on a single assembly flight.

Presented as Paper 91-2621 at the AIAA Guidance, Navigation, and Control Conference, New Orleans, LA, Aug. 12-14, 1991; received Sept. 23, 1991; revision received March 3, 1992; accepted for publication March 25, 1992.

*Research Engineer, Spacecraft Controls Branch. Member AIAA.
†Assistant Branch Head, Spacecraft Dynamics Branch. Senior Member AIAA.
‡Control and Dynamics Division; currently Research Engineer, ViGYAN, Inc., Hampton, VA. Member AIAA.

The study described in this paper is restricted to consideration of existing RMS hardware if possible, with minimal addition of new hardware only if necessary. The flight experiment computer and the distributed sensors proposed in the CSDL study would be eliminated in favor of using the existing Shuttle on-orbit computers for control-law implementation.

Damping Augmentation Methods

There are two distinct approaches to reduce residual motions of the RMS following commanded motions. One approach is to reduce the residual oscillations by using input command shaping techniques, as was done by Singer and Seering.[5] A second approach involves using output feedback of measurements of the system response to derive joint commands designed to damp the residual motions. An example of this approach is the work by Prakash et al.,[6] who used a detailed analytical model of the RMS to design model-based compensators. Other methods for robust controller design of flexible link arms and nonlinear control methods were suggested by Korolov and Chen[7] and Kreutz and Jamieson,[8] respectively.

The advantages of the input shaping approach is that accurate identification of plant parameters, such as frequency and damping, is not critical, and there is no knowledge requirement for the controller influence coefficients. One disadvantage is a significant phase lag between the desired input and corresponding motion of the RMS. This move time penalty is on the order of one period of the first mode of vibration. The operator commands the arm to stop, but the endpoint will continue to move for a few seconds. This results in the RMS not having the same "feel" as the current RMS when used by a trained operator and could be detrimental where precise positioning is required. Another disadvantage of command shaping is that it cannot reject unknown disturbances. For example, oscillations of the RMS that result from the Shuttle thruster firings cannot be damped by an input shaping method applied solely to the RMS.

The second approach of employing output feedback through a model-based controller to reduce vibration has been

selected for this paper. However, to use a model-based controller, an accurate model of the plant dynamics is required. This model can be obtained either through an extensive analytical model development or through system identification. In this paper, an identified model derived from a nonlinear simulation of the RMS (described below) is used. The advantages of output feedback are that it can reject unknown disturbances regardless of their origin, and the controller can be implemented in such a way as to not change the "feel" of the RMS to trained operators.

Feasibility Study Approach

The approach to the RMS active damping feasibility study is the following. First, a set of payloads and arm configuration combinations consistent with the types of payloads expected during Space Station Freedom assembly were defined. Second, RMS dynamics and operational characteristics were examined using the nonlinear Draper RMS Simulator (DRS) code.[9] The code, which is used routinely for predicting arm dynamic motions for on-orbit RMS operations, was obtained from CSDL for this purpose. The simulation code includes models of the RMS structural dynamics, joint servos, motors, gearboxes, and the software modules loaded in the Shuttle computers for RMS control. The determination of active damping augmentation feasibility involved the design and simulation of candidate damping augmentation control laws. For this purpose, system-identification methods were employed on output data from the DRS to identify linear state-space models which closely match the DRS response for specific commanded arm movements. With the linear control design models, various active control-law design concepts were evaluated, as were the requirements for feedback sensors to measure arm motions. The final step was the simulation of the active damping control laws in a modified version of the DRS to determine the effects of system nonlinearities and computer time delays.

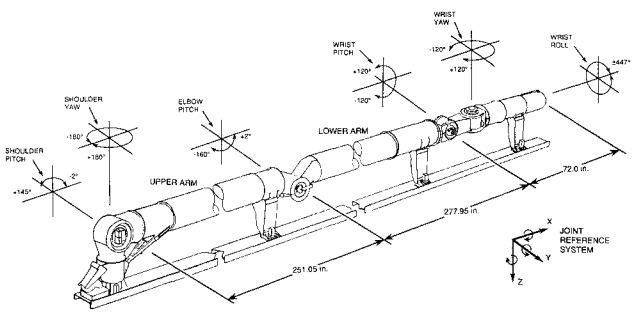

Fig. 1 Space Shuttle remote manipulator system (RMS).

II. Remote Manipulator System

System Description

Figure 1 illustrates the elements of the Space Shuttle RMS.[10] The system is a six-joint telerobotic arm controlled from a panel located on the aft flight deck of the Space Shuttle. These six joints are directly analogous to the joints and freedom of a human arm, defined as shoulder-yaw and pitch, elbow-pitch, and wrist-pitch, yaw, and roll. An end effector for grappling payloads is mounted at the free end of the arm. From the control panel and translational and rotational hand controllers, commands to move the arm are processed by the Shuttle computers and an interface unit to provide electrical signals to drive the joint servo motors. The actual joint servo commands that are generated depend on the selected operational mode, which can be either direct-drive, single-joint mode, one of four manual augmented modes, or an automatic control mode. The manual augmented mode is normally used for payload operations on-orbit, although the single-joint mode is used for RMS stowing and to avoid joint singularities. Joint angle position and motor shaft rate at each joint are measured by an encoder and tachometer, respectively.

Dynamic Response Studies

Three RMS configurations have been adopted for the current study. These configurations are shown in Fig. 2 with the Shuttle PAllet Satellite (SPAS) free-flyer spacecraft as an attached payload. The SPAS payload was used for the dynamic response studies since it is representative of a typical SSF assembly module. These configurations are actual configurations used during the deployment of the SPAS satellite on the STS-07 Shuttle mission. The first of these, referred to as position 1, is the position of the arm and payload just after release from the cargo bay attachments. Position 2 is the position of the arm and payload after being lifted from position 1 to a point which completely clears the sides of the cargo bay. Position 3 is the actual deployment positioning at the time of the SPAS release.

The time response data shown in Fig. 3 are typical of the kind of RMS motions encountered during normal arm maneuvers, as predicted by the DRS. The plots depict free responses following a 10-s single-joint rotation command to the shoulder-yaw joint with the other joint positions maintained by the RMS position-hold function. Shown are the lateral displacement of the free end of the arm, the shoulder-yaw joint angle encoder response, and the shoulder-yaw joint rate derived from the motor shaft tachometer. After the command to the RMS is removed, the peak-to-peak free oscillation at the tip of the arm is about 5 in., while the actual measured joint angle change during the same time is on the order of 0.1 deg. The discrete stepping of the encoder response is due to word length limitations in the Shuttle computer, indicating that the signal

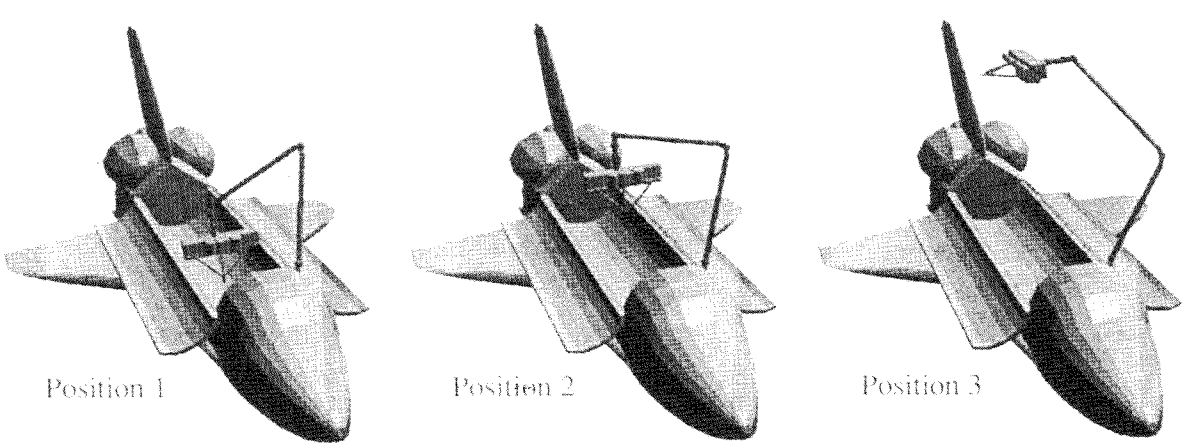

Fig. 2 RMS study configurations.

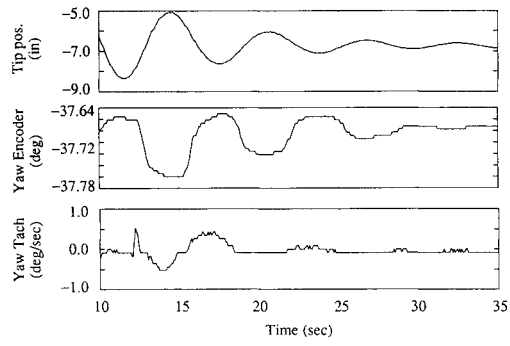

Fig. 3 Typical RMS response and sensor outputs.

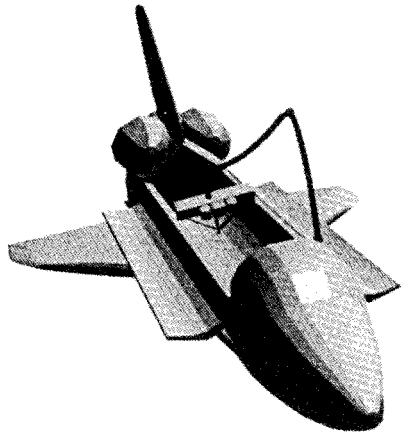

Fig. 4 RMS structural mode shape.

is at the limit of useful resolution. The yaw joint rate is on the order of 3.0 deg/s, and again has discrete stepping characteristics which limit the useful resolution of data. These types of responses are typical for the study configurations and SPAS payload and are an indication that the existing RMS sensors may not be adequate for active damping augmentation purposes. Because of this, the addition of another sensor in the form of a tip-mounted accelerometer was considered. The DRS simulation was used to predict three-axis response of an accelerometer package mounted on the SPAS payload. This simulated tip acceleration measurement was used in feedback studies to determine if additional sensor hardware would be beneficial for achieve damping augmentation of the RMS.

Global Mode Shape Visibility

Knowledge of the global mode shapes of the RMS was important in assessing the feasibility of active damping augmentation of the RMS. Since mode shapes change with arm geometry, the three configurations were studied. Appraisal was made of mode shape observability and controllability from the available sensor and actuator suites. Mode shape information was obtained using an eigenanalysis version of the DRS.

Figure 4 shows an exaggerated representation of the second mode of the RMS in position 1. The predicted frequency of this mode is 0.259 Hz. This mode shape includes a significant amount of upper and lower boom bending. Other RMS modes include significant amounts of joint flexibility and/or orbiter sidewall flexibility, with little boom bending contribution. To assess the relative contributions of each generalized coordinate in the state equations, the magnitudes of the eigenvector elements were plotted. Figure 5 is such a plot, showing the relative rotational contribution of states 1 through 13, and the relative displacement of states 14 through 17.

III. Controller Design and Evaluation

Linear single-input, single-output (SISO) state-space models were developed to investigate the damping improvement using local tachometer feedback to the respective joints and tip accelerometer feasibility studies. Multi-input, multi-output (MIMO) state-space models were developed to investigate multivariable state feedback controllers. The methods and results for both cases are presented below.

Single-Input, Single-Output Studies

System Identification

Linear SISO state-space models of the RMS were derived from DRS response data using linear system-identification methods. The data have been obtained for single-joint mode cases with the SPAS payload using the 3-s shoulder-yaw joint rate command pulse as the input, and either the joint tachometer or linear acceleration measurement at the tip of the arm as the output. Assuming a nominal model order of eight states corresponding to four vibration modes, frequency, damping, and influence coefficient parameters were selected to make the model best match the DRS response data in a least-squares sense. In all cases, the system-identification process was greatly complicated by the highly nonlinear characteristics of the actual joint hardware. The SISO system-identification results for the shoulder-yaw tachometer are shown in Fig. 6. The solid line represents the nonlinear DRS predicted response and the dotted line corresponds to the identified linear model response. The identified linear models were used to evaluate the effect of tachometer and accelerometer feedback on system modes (i.e., damping) through simple gain-loop closures.

Active Damping Results

Figures 7 and 8 show the RMS damping improvement as a function of a scaled gain parameter for feeding back the shoulder-yaw and pitch tachometer measurements, and tip acceleration measurement for position 1. The initial damping values for zero gain for the two joints are different because the joints excite and are able to control different structural modes. For both joints, feedback of the tachometer measurement initially results in a small increase in RMS damping. Feedback of the acceleration measurement in both cases shows larger increases in damping. Also shown in Fig. 7 is the result of tachometer feedback as predicted by the nonlinear DRS code, validating the linear model tachometer results. Data shown in Fig. 9 for the shoulder-pitch tachometer feedback in position

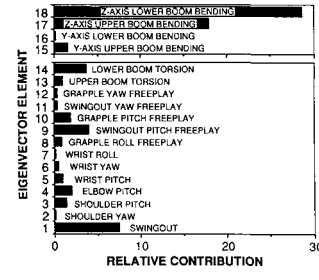

Fig. 5 RMS structural mode contributions.

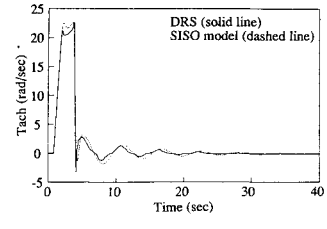

Fig. 6 SISO system-identification results for the shoulder-yaw tachometer.

3 illustrates the configurational dependence of RMS dynamics. Comparing Fig. 9 with Fig. 7, note the differences in open-loop damping and the effect of tachometer feedback for the two configurations. Feedback of tip acceleration is less affected by the configuration change and appears to be more desirable than tachometer feedback for active damping augmentation.

Multiple-Input, Multiple-Output Studies

The SISO studies investigated direct output feedback using tachometer and accelerometer measurements. Multivariable state feedback controllers were also investigated as part of the active damping feasibility study. These controllers were based on identified MIMO linear models of the RMS dynamics. The MIMO controller logic was implemented in the DRS nonlinear simulation so that candidate control laws could be evaluated including the effects of nonlinear arm dynamics, computer time delays, and existing RMS health and safety software functions.

The MIMO controllers are of the form

$$x_c(k+1) = A_c x_c(k) + B_c y(k)$$
$$u(k) = C_c x_c(k) + D_c y(k) \quad (1)$$

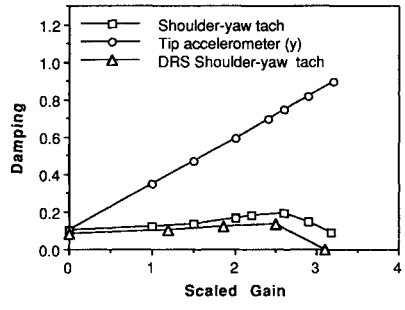

Fig. 7 Damping as a function of scaled gain for position 1 using the shoulder-yaw joint.

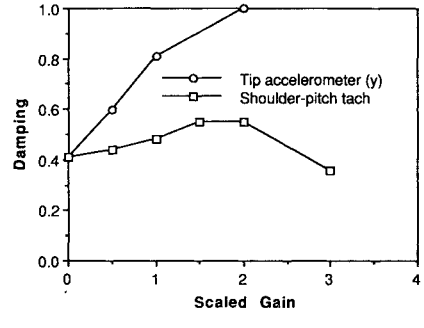

Fig. 8 Damping as a function of scaled gain for position 1 using the shoulder-pitch joint.

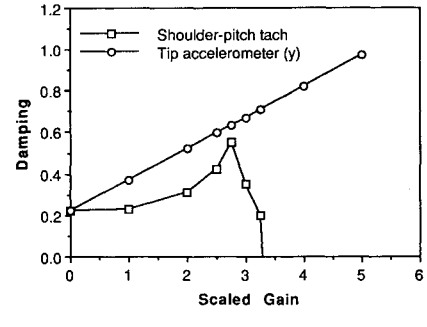

Fig. 9 Damping as a function of scaled gain for position 3 using the shoulder-pitch joint.

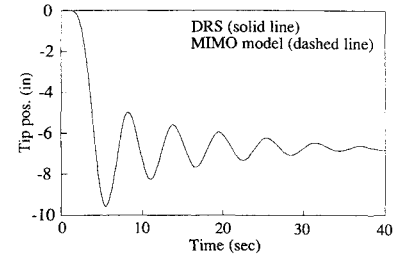

Fig. 10 MIMO system-identification results for the tip position (y axis).

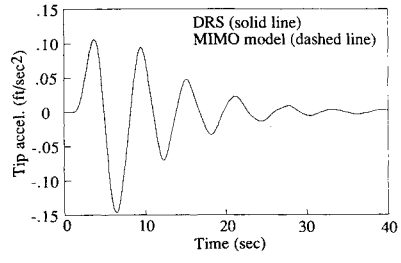

Fig. 11 MIMO system-identification results for the tip accelerometer (y axis).

where A_c is the compensator dynamics matrix; B_c the control distribution matrix; C_c the observation matrix; D_c the control feedthrough matrix; x_c the state vector; and y the measurement vector consisting of the six-joint encoder signals, the six-joint motor-rate signals, and three orthogonal RMS tip acceleration signals. The output vector u of the controller consists of six-joint rate commands.

System Identification

The technique used for MIMO system identification was the observer/Kalman filter identification method (OKID)[11,12] that has recently been developed at the NASA Langley Research Center. (The OKID method, in addition to identifying the state-space matrices A, B, C, and D, also identifies an observer gain matrix M for the system. This identified observer is used later for control-law design). Three models were derived, corresponding to the three study positions of the RMS. All three models had three inputs corresponding to the shoulder-yaw, shoulder-pitch, and elbow-pitch rate commands, and three outputs corresponding to the three-axis acceleration at the tip of the RMS. Each joint was given a 3-s pulse rate command, which was intended to excite the low-frequency modes. The response data was aggregated to allow the OKID algorithm to identify a single model representing the response of the RMS to any of the inputs. The three models are sixth order, corresponding to three structural modes. Prior to the system identification, the DRS simulation acceleration data were processed through a first-order low-pass filter with a break frequency of 0.2 Hz.

Results of the MIMO system identification are shown in Figs. 10 and 11. Shown are comparisons of the nonlinear DRS simulation response data with one of the MIMO identified models. Figure 10 shows the arm tip position following the 3-s pulse shoulder-yaw rate command (from 0 to 3 s in the plot) for position 1. In this figure both the DRS nonlinear simulator (solid line) and the identified linear model (dashed line) match so closely that the curves overlap. Figure 11 illustrates the y axis of the tip acceleration for both the DRS nonlinear simulator (solid line) and the identified linear model (dashed line) for the same 3-s pulse command. A summary of the identified frequency and damping of the three structural modes for the three study configurations is given in Table 1.

Table 1 Frequency and damping of identified modes

	Position 1		Position 2		Position 3	
Mode	Frequency, Hz	Damping	Frequency, Hz	Damping	Frequency, Hz	Damping
1	0.180	0.118	0.170	0.086	0.138	0.129
2	0.199	0.113	0.214	0.202	0.198	0.379
3	0.488	0.421	0.352	0.593	0.363	0.755

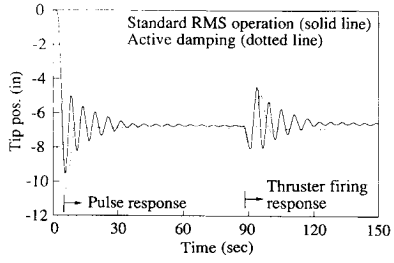

Fig. 12 Tip position following 3-s pulse command. After 90 s the Shuttle thrusters are fired for 6 s.

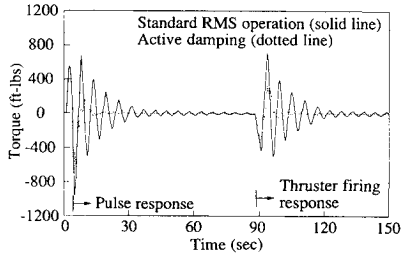

Fig. 13 Shoulder-yaw servo torque following 3-s pulse command. After 90 s the Shuttle thrusters are fired for 6 s.

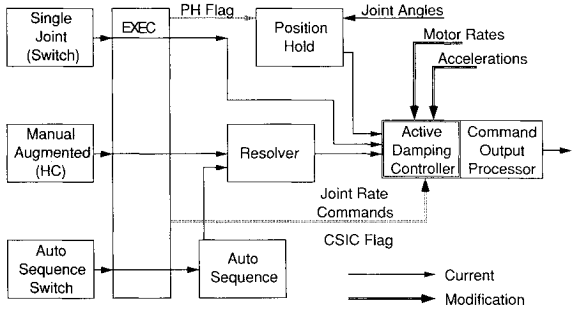

Fig. 14 Proposed controller implementation in Shuttle software.

Controller Design

The multivariable vibration suppression control law for each configuration was developed using the frequency weighted linear quadratic regulator (LQR) design method of Gupta.[13] Prior to the frequency-weighted LQR regulator design, a digital high-pass prefilter was added in series to the identified model to reject steady-state bias as would be encountered in feeding back accelerometer measurements in a real system. This filter had the digital form

$$N(z) = \frac{\tau_1 z + \tau_2}{\tau_3 z + \tau_4} \tag{2}$$

where the constants τ_1 through τ_4 have the values 0.9707, -0.9707, 1, and -0.9414, respectively. The values for this filter correspond to a first-order high-pass filter with a break frequency of 0.12 Hz. The identified model and prefilter are described by the state-space model

$$\begin{aligned} x(k+1) &= \hat{A}x(k) + \hat{B}u(k) \\ y(k) &= \hat{C}x(k) + \hat{D}u(k) \end{aligned} \tag{3}$$

For control purposes, a fixed gain regulator of the form

$$u(k) = -G\hat{x}(k) \tag{4}$$

was used, where u is the vector of joint rate command signals. The state estimate $\hat{x}$ was obtained from an observer of the form

$$\hat{x}(k+1) = \hat{A}\hat{x}(k) + \hat{B}u(k) + M[y(k) - \hat{C}\hat{x}(k)] \tag{5}$$

where y is the tip accelerometer measurement and the observer gain M was identified from the OKID system-identification method.

To obtain the optimal gain G, the model with the prefilter was used in a frequency weighted LQR design with a weighted cost function of the form

$$J = \sum_{k=0}^{N} y^T Q y + u^T R u \tag{6}$$

where Q is the output weight matrix and R the control weighting matrix. The numerical values of Q and R were determined using an iterative design procedure on the linear model that avoided actuator saturation. The final values used in the design are $Q = \text{diag}\{0.002\ 0.002\ 0.002\}$ and $R = \text{diag}\{0.01\ 0.01\ 0.05\}$. Using

$$y = \hat{C}\hat{x} + \hat{D}u \tag{7}$$

the performance index, Eq. (5), was recast:

$$J = \sum_{k=0}^{N} \hat{x}^T \hat{C}^T Q \hat{C}\hat{x} + 2\hat{x}^T \hat{C}^T Q \hat{D}u + u^T(\hat{D}^T Q \hat{D} + R)u \tag{8}$$

The optimal feedback gain G that minimizes the performance index J in Eq. (8) was found using Matrix$_x$[14] software tools.

Active Damping Results

The multivariable LQR controller with observer was evaluated on the DRS nonlinear simulation. The tip position following a 3-s shoulder-yaw pulse rate command is shown in Fig. 12. In addition, after 90 s, a Shuttle thruster roll doublet firing was simulated for 6 s. The solid line represents standard RMS operation, and the dotted line represents actively damped performance. The time required to damp the tip oscillation to ± 1 in. is decreased by a factor of 3. The shoulder-yaw servo torque following the 3-s shoulder-yaw pulse rate command is shown in Fig. 13. The solid line represents simulated standard RMS operation, and the dotted line represents closed-loop performance. In this time history, the controller has the effect of reducing the applied torque by a factor of 2. This provides the added potential benefit of reducing the structural stress in the arm following routine maneuvers involving either joint commands or Shuttle thruster firings.

IV. Controller Implementation in RMS Software

Based on the recommendations of CSDL, a potential means of implementing an active damping augmentation controller in the Shuttle computer software was identified. This strategy, illustrated in Fig. 14, allows use of all existing RMS health and safety monitoring functions in an effort to simplify flight development work. The active damping controller would be a software module that acts as a preprocessor to the existing RMS command output processor. It would be turned on and off by the executive function of the existing software by a flag that would activate the controller when RMS joint move commands are zeroed. Using motor rate and/or acceleration feedback measurements, the controller would damp the free response of the arm to some level, at which time the normal position-hold function of the arm would be activated. With this implementation, the active damping function of the controller could be expanded to damp RMS motions following Shuttle thruster firings as well.

V. Concluding Remarks

An analytical study to determine the feasibility of actively augmenting the damping of the Shuttle remote manipulator system has been summarized. Single-input, single-output and multi-input, multi-output linear models were identified and used to design direct output feedback and multivariable controllers. The controller and logic were evaluated in a nonlinear simulation, which included the effects of nonlinear arm dynamics, computer time delays, and existing Shuttle health and safety software functions. Based on initial results, active damping of the remote manipulator system appears feasible using the existing joint actuators and Shuttle computers and software. However, some additional feedback sensors in the form of accelerometers located at the tip of the arm are required.

The controller developed for this system does not change or delay the trained operator input command to move the arm, thus, the "feel" of the arm has not been altered. In addition, the controller incorporates output compensation to ensure that the robotic manipulator is in the same final position as when the vibration suppression strategy was initiated. The multi-input, multi-output control system, when evaluated on the nonlinear simulation, demonstrated significant improvement over the present arm performance: 1) the damping level is improved by a factor of 3; and 2) peak joint torque is reduced by a factor of 2 following Shuttle thruster firings. Future evaluation of this controller is planned on the Shuttle Engineering Simulator at the NASA Johnson Space Center. Based on the results of the simulations, the Shuttle community will decide whether or not it is desirable to advocate a flight demonstration.

References

[1]Bole, C. D., and Foiale, R. R., "RMS Mission Histories," NASA JSC-23504, March/April 1989, pp. 13, 16.

[2]Demeo, M. E., "Remote Manipulator System (RMS)-Based Controls-Structure Interaction (CSI) Flight Experiment Feasibility Study," NASA CR 181952, Jan. 1990.

[3]Demeo, M. E., Fontana, A., and Bains, E. M., "Shuttle Remote Manipulator System (RMS)-Based Controls-Structures Interaction Flight Experiment," Fourth NASA/DOD Conf. on Controls-Structures Interaction Technology, Orlando, FL, Nov. 1990.

[4]Lamb, B. A., and Nowlan, D. R., "Benefits of Control Structure Interaction (CSI) Technology to Space Station Assembly by Flexible Robotic Systems (RS)," NAS1-18763, Nov. 1989.

[5]Singer, N. C., and Seering, W. P., "Preshaping Command Inputs to Reduce System Vibration," *Journal of Dynamic Systems, Measurement, and Control,* Vol. 112, March 1990, pp. 76–82.

[6]Prakash, O., Adams, N. J., and Appleby, B. D., "Multivariable Control of Space Shuttle Remote Manipulator System," *Proceedings of the AIAA Guidance, Navigation, and Control Conference* (New Orleans, LA) AIAA, Washington, DC, 1991, pp. 1923–1931.

[7]Korolov, V. V., and Chen, Y. H., "Controller Design Robust to Frequency Variation in a One Link Flexible Robot Arm," *Journal of Dynamic Systems, Measurement, and Control,* Vol. 111, 1989, pp. 9–14.

[8]Kreutz, K., and Jamieson, R. S., "Linearization of Robot Manipulators," *NASA Technical Brief,* Vol. 11, No. 8, item #114, 1987.

[9]Gray, C., et al., "Validation of the Draper RMS Simulation (DRS) Against Flight Data," Charles Stark Draper Lab., CSDL-R-1755, Vols. 1–2, Cambridge, MA, April 1985.

[10]"Space Shuttle Payload Accommodations," NASA Johnson NSTS 00700, Vol. XIV, Appendix 8, Revision J, Houston, TX, Jan. 1988.

[11]Phan, M., Horta, L. G., Juang, J.-N., and Longman, R. W., "Linear System Identification Via an Asymptotically Stable Observer," NASA TP 3164, June 1992.

[12]Juang, J.-N., Horta, L. G., Phan, M., and Longman, R. W., "Identification of Observer and Kalman Filter Markov Parameters: Theory and Experiments," *Proceedings of the AIAA Guidance, Navigation, and Control Conference* (New Orleans, LA), AIAA, Washington, DC, 1991, pp. 1195–1207; also *Journal of Guidance, Control, and Dynamics* (to appear).

[13]Gupta, N. K., "Frequency-Shaped Cost Functionals: Extensions of Linear-Quadratic Gaussian Design Methods," *Journal of Guidance and Control,* Vol. 3, No. 6, 1980, pp. 529–535.

[14]*MATRIX$_X$ Control Design Module,* 7th ed., Integrated Systems Inc., Santa Clara, CA, Jan. 1990.